Key Role of Nitrate in Phase Transitions of Urban Particles:

Sun, Jiaxing; Liu, Lei; Xu, Liang; Wang, Yuanyuan; Wu, Zhijun; Hu, Min; Shi, Zongbo; Li, Yongjie; Zhang, Xiaoye; Chen, Jianmin; Li, Weijun

DOI:
10.1002/2017JD027264

AGU PUBLICATIONS

JGR

Journal of Geophysical Research: Atmospheres

RESEARCH ARTICLE
10.1002/2017JD027264

Key Points:
- Laboratory-generated ammonium sulfate-ammonium nitrate (AS-AN) particles undergo two stage deliquescence and one stage efflorescence
- Aqueous shell and solid core occur on urban haze particles with relative humidity at 60–80%
- AN content mainly determines the MDRH of urban haze particles, and AS mainly determines DRH

Supporting Information:
- Supporting Information S1

Correspondence to:
W. Li,
liweijun@zju.edu.cn

Citation:
Sun, J., Liu, L., Xu, L., Wang, Y., Wu, Z., Hu, M., … Li, W. (2018). Key role of nitrate in phase transitions of urban particles: Implications of important reactive surfaces for secondary aerosol formation. *Journal of Geophysical Research: Atmospheres*, *123*. https://doi.org/10.1002/2017JD027264

Received 7 JUN 2017
Accepted 31 DEC 2017
Accepted article online 5 JAN 2018

Key Role of Nitrate in Phase Transitions of Urban Particles: Implications of Important Reactive Surfaces for Secondary Aerosol Formation

Jiaxing Sun[1,2], Lei Liu[2], Liang Xu[2], Yuanyuan Wang[2], Zhijun Wu[3], Min Hu[3], Zongbo Shi[4], Yongjie Li[5], Xiaoye Zhang[6], Jianmin Chen[7], and Weijun Li[1]

[1]Department of Atmospheric Sciences, School of Earth Sciences, Zhejiang University, Hangzhou, Zhejiang, China, [2]Environment Research Institute, Shandong University, Jinan, Shandong, China, [3]State Key Joint Laboratory of Environmental Simulation and Pollution Control, College of Environmental Sciences and Engineering, Peking University, Beijing, China, [4]School of Geography, Earth and Environmental Sciences, University of Birmingham, Birmingham, UK, [5]Department of Civil and Environmental Engineering, Faculty of Science and Technology, University of Macau, Taipa, Macau, China, [6]Key Laboratory of Atmospheric Chemistry of CMA, Institute of Atmospheric Composition, Chinese Academy of Meteorological Sciences, Beijing, China, [7]Shanghai Key Laboratory of Atmospheric Particle Pollution and Prevention, Department of Environmental Science and Engineering, Fudan University, Shanghai, China

Abstract Ammonium sulfate (AS) and ammonium nitrate (AN) are key components of urban fine particles. Both field and model studies showed that heterogeneous reactions of SO_2, NO_2, and NH_3 on wet aerosols accelerated the haze formation in northern China. However, little is known on phase transitions of AS-AN containing haze particles. Here hygroscopic properties of laboratory-generated AS-AN particles and individual particles collected during haze events in an urban site were investigated using an individual particle hygroscopicity system. AS-AN particles showed a two-stage deliquescence at mutual deliquescence relative humidity (MDRH) and full deliquescence relative humidity (DRH) and three physical states: solid before MDRH, solid-aqueous between MDRH and DRH, and aqueous after DRH. During hydration, urban haze particles displayed a solid core and aqueous shell at RH = 60–80% and aqueous phase at RH > 80%. Most particles were in aqueous phase at RH > 50% during dehydration. Our results show that AS content in individual particles determines their DRH and AN content determines their MDRH. AN content increase can reduce MDRH, which indicates occurrence of aqueous shell at lower RH. The humidity-dependent phase transitions of nitrate-abundant urban particles are important to provide reactive surfaces of secondary aerosol formation in the polluted air.

Plain Language Summary Recently, aerosol water has received more attention because heterogeneous reactions of SO_2, NO_2, and NH_3 on wet particles accelerate the severe haze formation in north China. Ammonium sulfate and ammonium nitrate (AS-AN) are key components of fine urban particles. Especially, nitrate concentration keeps increasing in polluted air in China. Our study indicates that the increase of AN content promotes the occurrence of aqueous shell at lower RH. Here we find that most of urban particles generally keep solid core and aqueous shell at RH = 60–80% and aqueous phase at RH > 80%. These findings can clearly explain the role of nitrate in phase transitions and make up the discussion about heterogeneous reactions on particle surfaces during the severe hazes in north China. Humidity-dependent phase states of particles are useful for interpreting the secondary aerosols' formation in severe hazes as well as in modeling studies.

1. Introduction

The hygroscopicity of atmospheric particles can determine how particles change with varying relative humidity (RH). Thus, RH has a key impact on the physical properties of particles, including size, morphology, and wavelength-dependent refractive indices (Freney et al., 2010; L. Zhang et al., 2015; Wise et al., 2009). In addition, water uptake of atmospheric aerosols influences their atmospheric lifetimes, reactivity, effects on air quality, and, ultimately, their effects on human health (Ervens, 2015; Hodas, Sullivan, et al., 2014; Liu et al., 2014).

Sulfate, nitrate, ammonium (i.e., ammonium sulfate (AS) and ammonium nitrate (AN)), and organics are the main components in urban haze particles, contributing 30–77% of $PM_{2.5}$ mass in northern China (Huang et al., 2014). Effects of organic matter on water uptake of inorganic components depend on organic

species, amounts, solubility, and oxidation degree (Hodas, Zuend, et al., 2014; Zardini et al., 2008). When some organic compounds are internally mixed with secondary inorganic particles, hygroscopic inorganic aerosols still determine particle hygroscopicity such as deliquescence relative humidity (DRH), efflorescence relative humidity (ERH), and growth factor (GF; Jing et al., 2016; Peckhaus et al., 2012). Therefore, the study of the hygroscopicity of inorganic mixed system is a necessary step to determine phase transitions of urban particles having large fractions of inorganic aerosols. Secondary sulfate and nitrate are the main inorganic hygroscopic aerosol components that determine DRH and ERH of atmospheric particles (Kuang et al., 2016; X. Wang et al., 2014). Li et al. (2016) shows that AS and AN constituents in internally mixed particles provide important particle surfaces during the severe haze events. In particular, AN is known as a highly hydrophilic aerosol component (Hodas, Sullivan, et al., 2014). In the past 10 years, nitrate concentrations in $PM_{2.5}$ keep increasing in the polluted areas of east China (X. Y. Zhang et al., 2015), and they sometimes are even higher than AS in urban areas (Lu et al., 2015; Sun et al., 2013). Therefore, it is necessary to understand the key role of nitrate in the hygroscopic properties of haze particles in urban areas of north China.

Recently, some studies found that heterogeneous reactions in aerosol water are a significant mechanism for haze formation in north China (G. J. Zheng et al., 2015; Y. Wang et al., 2014). Both field measurements and modeling studies supported that rapid sulfate and nitrate formation from SO_2 and NO_2 were from heterogeneous reactions in the liquid surface of haze aerosols (Cheng et al., 2016; Wang et al., 2016). In addition, G. J. Zheng et al. (2015) found that both molar ratio of sulfate to the sum of sulfate and SO_2 and nitrate to the sum of nitrate and NO_2 were around 0.1 under dry conditions but increased to around 0.34 and 0.28 at 70–80% RH, respectively. Wang et al. (2016) showed that sulfate formation underwent an exponential increase with RH, with sulfate to SO_2 ratio increase from less than 0.1 when RH $\leq$ 20% to 1.1 when RH $>$ 90% during haze episodes. The heterogeneous reaction rates on particle surfaces have been assumed to depend on RH (Fairlie et al., 2010; Stutz et al., 2004). All these studies illustrated that heterogeneous reaction rates were related to RH changes, but it is unclear what the role of particle phase changes is in the processes during the urban haze events in northern China. Kuang et al. (2016) proposed that ambient particles in the North China Plain deliquesced into the aqueous phase with RH of 73–81%. However, the study only observed the deliquescence phase transition but could not obtain precise phase changes through nephelometers. This study will focus on understanding the phase states of secondary particles that are dependent on humidity, which is the key factor controlling atmospheric heterogeneous reaction rates. We will discuss the role of nitrate in phase transitions of urban particles and how these transitions can influence heterogeneous reactions on particle surfaces during the severe haze events in North China.

2. Experimental

Eleven solutions with different molar mixing ratios of AS and AN (X_{AN} = 0, 0.1, 0.2, 0.3, 0.4, 0.5, 0.6, 0.7, 0.8, 0.9, 1) (AS $>$ 99.5% purity; AN $>$ 99.0% purity) were prepared in the laboratory (Table S1 in the supporting information). Furthermore, particles from 11 AS-AN mixed solutions were generated using an aerosol atomizer within N_2 (99.999% purity) gas and deposited onto silicon wafers.

Haze particle samples were collected on the roof of a six-floor building on the campus of Shandong University, located among commercial and residential areas of Jinan, northern China. Aerosol samples were collected both onto copper transmission electron microscope (TEM) grids coated with carbon film and silicon wafers using a DKL-2 single particle sampler with a single-stage cascade impactor equipped with a 0.3 mm diameter jet nozzle at a flow of 1.0 L/min. The collection efficiency of the impactor is 50% for particles with an aerodynamic diameter of 0.1 μm and a density of 2 g cm^{-3}. The sampling duration was 10 s. Then we placed the samples in sealed, dry, plastic capsules to prevent contamination. Finally, the samples were stored in a desiccator at 20°C and 20 ± 3% RH and analyzed later on.

In this study, an individual particle hygroscopicity (IPH) system was built to investigate the hygroscopic properties of individual particles at different RH. The experimental process is composed of three steps: (1) introducing N_2 gas with controlled flow by a mass flow controller into a chamber; (2) mounting the TEM grid or silicon wafer with particles on the bottom of an environmental microscopic cell (Gen-RH Mcell, UK), which can change RH and keep a constant temperature of 20°C; and (3) taking images at different RH through an optical microscope (Olympus BX51M, Japan) with a camera (Canon 650D). A similar experimental setup is described elsewhere (Ahn et al., 2010). The pure NaCl crystal particles with the size range of 0.5–20 μm

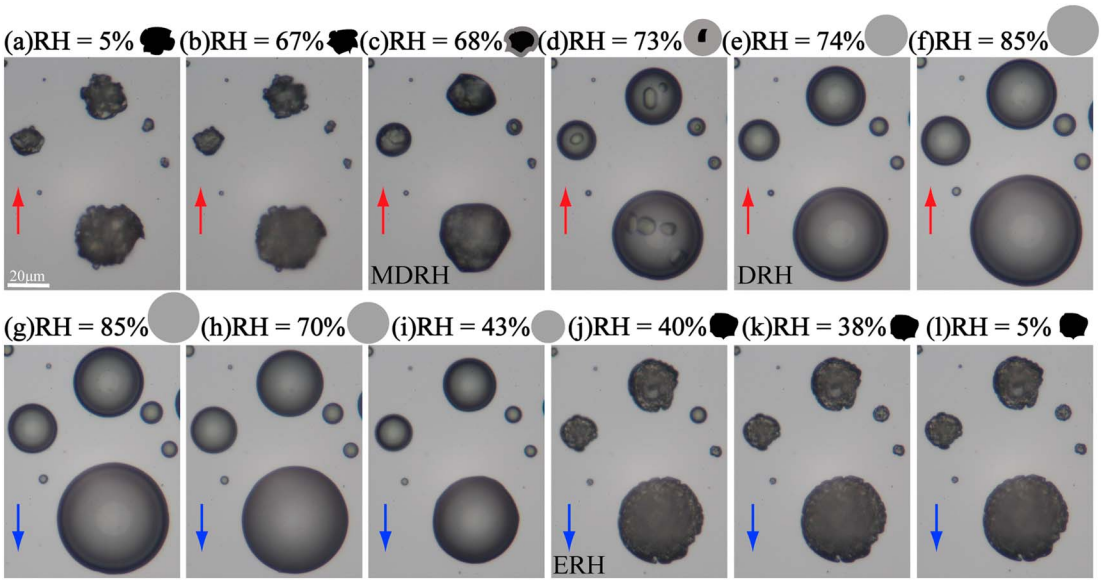

Figure 1. Optical images of AS-AN particles with a mixing ratio of AN:AS = 6:4 (X_{AN} = 0.6) in different RH at T = 293.15 K. (a–f) Particles' hygroscopic growth during hydration from 5% to 85% RH. Up arrow (↑) represents RH increase. (g–l) Particles' shrinkage during dehydration from 85% to 5% RH, in the same image field. Down arrow (↓) represents RH decrease.

were made in the laboratory and collected on silicon wafer substrate. Hygroscopic behaviors of these cubic NaCl particles tested the IPH system at different RH values from 3% to 94%. All the particles had DRH at 75%, which is consistent with the theoretical DRH (Figure S1). In this study, 11 laboratory-generated samples and two haze samples were chosen to observe particle hygroscopic growth in the IPH system. The images taken by the IPH system were used to compare their morphology and size at different RH values (e.g., Figure 1).

Composition, mixing state, and morphology of haze particles collected on TEM grids were further examined by a JEOL JEM-2100 transmission electron microscope operated at 200 kV with energy-dispersive X-ray spectrometry. The information can be used to explain the hygroscopic behavior of individual haze particles in the IPH system.

Hourly mass concentrations of water soluble ions during haze episodes were measured by an online Monitor for AeRosols and GAses in ambient air (MARGA, ADI20801, Applikon-ECN, Netherlands). We took AS and AN values during the sampling hour and then calculated the molar fractions of AN.The thermodynamic model Extended Aerosol Inorganic Model (E-AIM; http://www.aim.env.uea.ac.uk/aim/aim.php; Clegg et al., 1998) was used to predict the mutual deliquescence relative humidity (MDRH; i.e., DRH when the first deliquescence transition occurs; Wexler & Seinfeld, 1991) and DRH (i.e., when the full deliquescence transition occurs) values for AS-AN particles. We also obtained the GF of AS-AN particles using the E-AIM model. GF is an important parameter to quantify the size change of particles during hydration and dehydration (Figure 2). Particle GF is defined as

$$\mathrm{GF(RH)} = \frac{D(\mathrm{RH})}{D0}$$

D(RH) is the diameter of particles at a given RH and D_0 is the diameter of dry particles at 5% RH.

3. Results and Discussion

3.1. DRH and ERH of AS and AN Particles

DRH and ERH of AS particles were 81% and 47 ± 1% at 20°C (Figure 2a), consistent with DRH at 80 ± 1% and ERH at 31–48% reported by Martin (2000) and Onasch et al. (1999). AS particles underwent a shrinkage before 80% RH in experiments (Figure 2a). Some investigators have proposed that structural rearrangement by water vapor interacting with partial crystal surfaces led to this particle shrinkage (Ahn et al., 2010; Mikhailov et al., 2004). Moreover, the interactions of particles and substrate influence particles' shrinkage

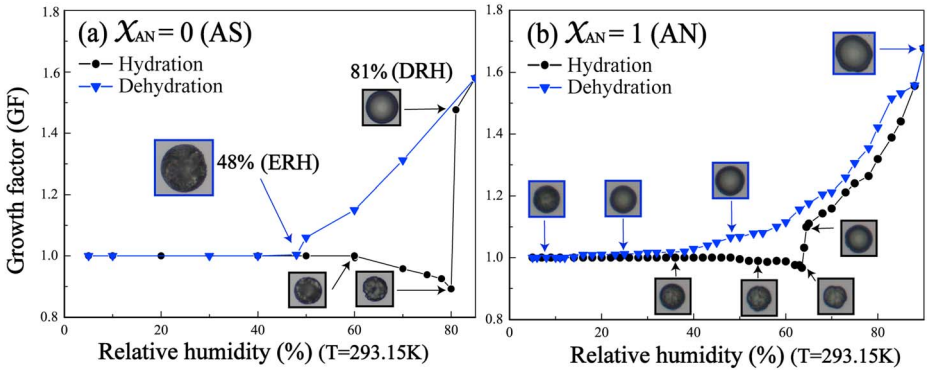

Figure 2. Growth factor (GF) of pure (a) AS and (b) AN particles as a function of RH (T = 293.15 K). Black circles represent hydration; blue triangles, dehydration.

should not be excluded because Wise et al. (2008) found that a significant amount of water is associated with the particles prior to deliquescence using environmental TEM. Through the whole hydration and dehydration cycles, AN particles likely kept droplet-like spherical morphology based on their smooth surface on the substrate (Figure 2b). Therefore, we speculated that there must be water presented in particles at all RH. It should be noticed that slight size increase of AN particles occurred at ~64% RH even though there was no obvious phase change compared to the AS. Overall, we cannot judge a distinct DRH of AN particles due to the uniform phase state. During dehydration (Figure 2b), AN particles continuously retained a droplet-like spherical shape even with RH values as low as 5%; furthermore, size of the AN particles decreased gradually without an abrupt change. Therefore, AN particles did not undergo a crystallization transition even at low RH. These hygroscopic properties of AN particles are consistent with the results from other methods such as hygroscopic tandem differential mobility analyzers (HTDMA), nephelometry, and infrared extinction spectroscopy (Cziczo & Abbatt, 2000; Dougle et al., 1998; Hu et al., 2011).

3.2. Direct Observations of the Hygroscopic Behavior of AS-AN Particles

3.2.1. Hydration/Dehydration of AS-AN Particles

Figures 1 and 3c show the change in size and morphology of the AS-AN particles (X_{AN} = 0.6) during hydration and dehydration. During hydration, shrinkage of particles occurred at RH = 67% (Figures 1b and 3c). When RH increased up to 68%, the surface of the AS-AN particles started to change from solid into liquid (Figure 1c). Based on our observations, particles (X_{AN} = 0.6) deliquesced firstly at MDRH and then fully deliquesced at DRH. At the MDRH, particle surface changed from having an irregular to spherical at RH = 68% (Figure 1c), which leads to particle size starting growth (Figure 3c). At a DRH of 74%, particles completely changed into solutions (Figure 1e) with a large increase in size. Thereafter, particle sizes grew continuously as RH increases (Figure 3c).

The two-stage deliquescence (i.e., MDRH and DRH) of AS-AN particles were observed in nine mixing ratios (X_{AN} = 0.1–0.9) during hydration (Figure 3). It should be noted that the MDRH of AS-AN particles with different mixing ratios showed different values: 68% for X_{AN} = 0.1–0.6 (Figures 3a–3c), 67% for X_{AN} = 0.7 (Figure 3d), 64% for X_{AN} = 0.8 (Figure 3e), and 63% for X_{AN} = 0.9 (Figure 3f). The DRH of AS-AN particles increased with the decreasing content of AN, approaching the DRH of pure AS particles: X_{AN} = 0.1–0.9, DRH at 80%, 79%, 78%, 77%, 76%, 74%, 72%, 68%, and 66%, respectively (Figures 3a–3f). The tendency of the GF curves obtained from the experiments and the E-AIM model is similar during hydration (Figures 3a–3f). The result is consistent with a recent study by Morris et al. (2016) who showed that the GF values of wet-deposited particles after DRH derived from two-dimensional optical images are similar with results derived both from three-dimensional images in atom force microscopy and HTDMA measurement. Meanwhile, we should notice that although the E-AIM model successfully simulated the observed GF, it still could not well predict particle shrinkage before its MDRH (Figure 3).

Based on particle morphological and size changes, we can obtain their ERH during dehydration (Figures 1g–1l). We observed that the ERH of different AS-AN particles with an X_{AN} of 0.6 range from 38% to 40%, with an average of 39%. We did not observe obvious crystallization of individual AS-AN particles

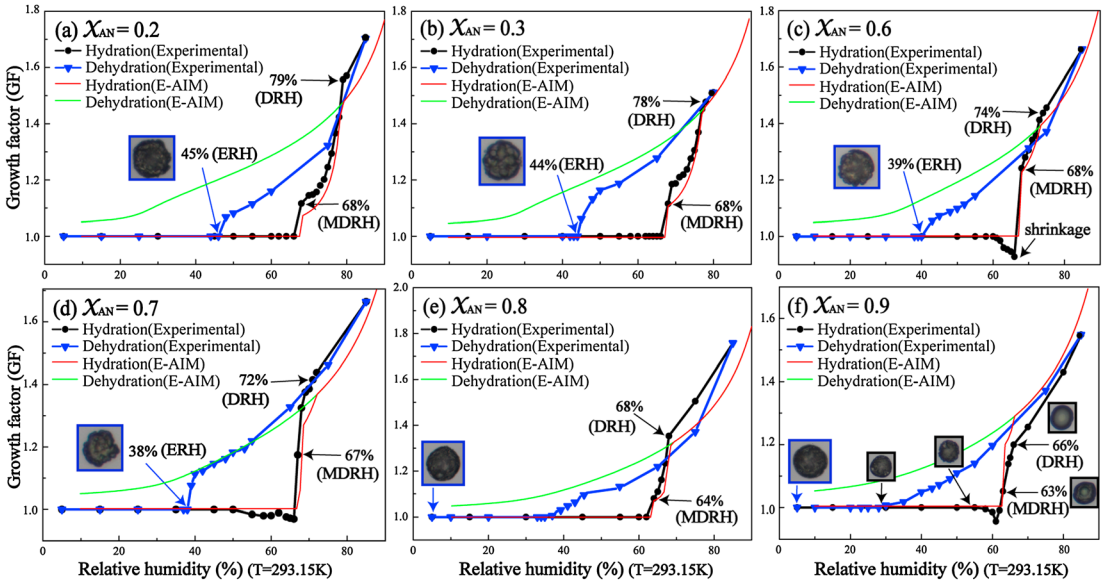

Figure 3. Growth factor (GF) of AS-AN particles in different mixing ratios ((a–f) X_{AN} = 0.2, 0.3, 0.6, 0.7, 0.8, 0.9) as a function of RH (T = 293.15 K). Black circles represent hydration; blue triangles, dehydration. The red curves were GF values derived from the E-AIM model during hydration; the green curves were during dehydration.

with X_{AN} between 0.8 and 0.9 even when the RH was as low as 5% (Figures 3e and 3f). During dehydration, the mixed AS-AN particles (X_{AN} = 0.8 and 0.9) kept solid-like round morphology with unsmooth surface at 5% RH, which was different from the droplet-like spherical shape observed for pure AN particles. In this study, we were unable to identify whether there was condensed water in these solid-like particles. During dehydration, the size of these two mixed AS-AN particles behaved similarly to pure AN particles, which decreased gradually without an abrupt change. A similar result has been reported by Dougle et al. (1998) who found that no crystallization occurred when the mole ratios of AN to AS were above 0.683, based on absence of abrupt change in light scattering measured by nephelometers. Our study showed that once $X_{AN} \leq 0.7$, AS-AN particles displayed a one-stage efflorescence transition during the dehydration: 45% RH as ERH for X_{AN} = 0.1, 45% for X_{AN} = 0.2, 44% for X_{AN} = 0.3, 43% for X_{AN} = 0.4, 42% for X_{AN} = 0.5, 39% for X_{AN} = 0.6, and 38% for X_{AN} = 0.7 (Figures 3a–3f). The ERH of AS-AN particles decreased with the increasing X_{AN}. Meanwhile, GF values derived from E-AIM model were usually higher than experimental values. Efflorescence is a kinetic-driven process that depends on a range of complex factors such as particle mixing state and components interactions (Martin, 2000), therefore making it difficult for the E-AIM model to accurately predict particle ERH and GF during dehydration.

3.2.2. Deliquescent and Efflorescent Phase Diagrams of AS-AN Particles

The IPH system provided the morphological and size changes of particles, but it could not provide any component information about the intermediate phases. In this study, DRH values of AS-AN particles at different mixing ratios were predicted by the E-AIM model to decrease with X_{AN}; E-AIM also predicted three different MDRH values: 69% for X_{AN} = 0.01–0.66, 68% for X_{AN} = 0.67–0.75, and 64% for X_{AN} = 0.76–0.99. These results are similar to those observed in the IPH system (Figure 4a). However, some other studies proposed only one MDRH of two-component inorganic particles (Ge et al., 1998; Gupta et al., 2015; Wexler & Seinfeld, 1991). Recently, Fong et al. (2016) observed that the MDRH of mixed inorganic system varied slightly with the variation of mixture's mole ratio. Data obtained from the IPH system on the MDRH and DRH enabled us to construct the phase diagram, which shows solid-aqueous equilibrium phase transition during hydration (Figure 4a). The diagram was divided into three parts according to the physical states of AS-AN particles.

AS-AN particles are in solid phase when RHs are lower than MDRH. Through the simulation of E-AIM model, we obtain the aerosol components of solid particles. When $X_{AN} \leq 0.6$, particles are composed of AS and $2NH_4NO_3{\cdot}(NH_4)_2SO_4$; when X_{AN} = 0.7, particles contain $2NH_4NO_3{\cdot}(NH_4)_2SO_4$ and $3NH_4NO_3{\cdot}(NH_4)_2SO_4$ components; and when $X_{AN} > 0.7$, solid particles contain AN and $3NH_4NO_3{\cdot}(NH_4)_2SO_4$.

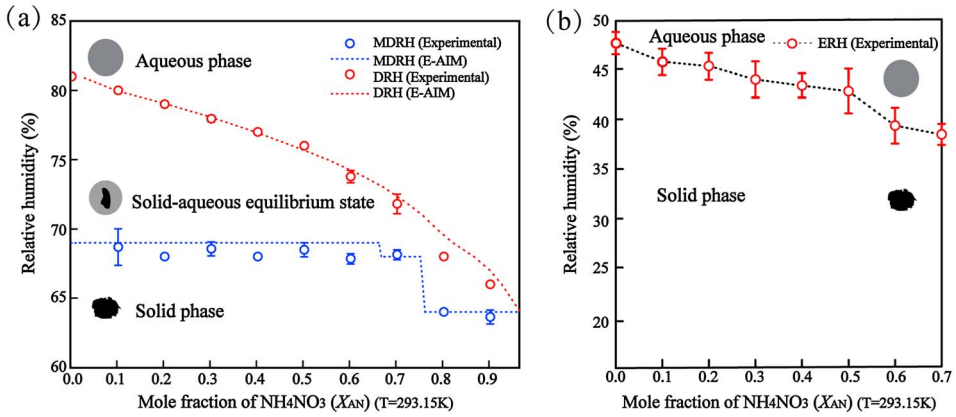

Figure 4. Phase diagrams of AS-AN particles during (a) hydration and (b) dehydration as a function of X_{AN} (T = 293.15 K). (a) Experimental measured MDRH and DRH are represented in open blue and red circles, respectively. E-AIM simulated MDRH ($MDRH_1$ = 69% when X_{AN} = 0.01–0.66; $MDRH_2$ = 68% when X_{AN} = 0.67–0.75; $MDRH_3$ = 64% when X_{AN} = 0.76–0.99) and DRH are given in blue and red dotted lines, respectively. Three physical states: solid phase, solid-aqueous equilibrium state, and aqueous phase are divided during hydration. (b) Open red circles represent experimental measured ERH derived from the IPH system. Solid phase and aqueous phase are given during dehydration.

AS-AN particles are in solid-aqueous equilibrium state when RHs are higher than MDRH and lower than DRH. Solid-aqueous equilibrium state is a transition region where particle partially dissolves into aqueous solution but do not yet become deliquesced completely. AS-AN particles keep in a solid-aqueous equilibrium state between the MDRH and DRH. Figure 1d shows that particles in this physical state consisted of a solid core with an aqueous shell (e.g., Figure 1d). The E-AIM model shows the dissolution process of solid particles. When $X_{AN} \leq 0.6$, partial AS keeps in solid phase while other components dissolve into solution; when X_{AN} = 0.7, with absorption of water, remanent solid constituent $2NH_4NO_3{\cdot}(NH_4)_2SO_4$ gradually dissolves and then partial AS remains in solid phase; when $X_{AN} > 0.7$, with RH increase, $3NH_4NO_3{\cdot}(NH_4)_2SO_4$ solid remains, then $2NH_4NO_3{\cdot}(NH_4)_2SO_4$ remains, and finally AS remains in solid in this region.

When RHs are higher than DRH, solid particles completely dissolve into aqueous phase.

Therefore, AS-AN particles experienced a significant intermediate solid-aqueous equilibrium state between MDRH and DRH, which is different from single component particles with an abrupt deliquescence phase transition (Martin, 2000).

Figure 4b shows the measured ERH of AS-AN particles as a function of molar fraction of AN (X_{AN}). As X_{AN} decreased, ERH of particles increased and approached to the ERH of an AS particle. Based on a one-stage efflorescence phase transition, a phase diagram showing liquid to solid phase transition has two phases (Figure 4b):

Particles are in solid phase when RHs are lower than ERH;
Particles are in aqueous phase when RHs are higher than ERH.

3.3. Direct Observations of Hygroscopic Behavior of Urban Haze Particles

Two individual particle samples were collected during two typical haze episodes in urban Jinan of north China. The molar fractions of AN were calculated to be X_{AN} = 0.51 (sample A1) and X_{AN} = 0.83 (sample A2), which can represent the ordinary haze and AN-abundant urban haze events in China (G. J. Zheng et al., 2015; Lu et al., 2015; Sun et al., 2013; Yuan et al., 2015). We chose two samples for hygroscopicity measurements with the IPH system. In light of the limitation of optical microscopy, the IPH system can clearly observe hygroscopic behaviors of individual particles with size larger than 0.5 μm. Laskina et al. (2015) showed that hygroscopic properties of particles with size larger than 100 nm were determined by their components. During the severe hazes in north China, 90% of particles belong to the accumulation mode (i.e., larger than 100 nm; Li et al., 2011). Therefore, we believe our results in this study can represent the hygroscopic behavior of urban haze particles. We observed that haze particles started to absorb water at

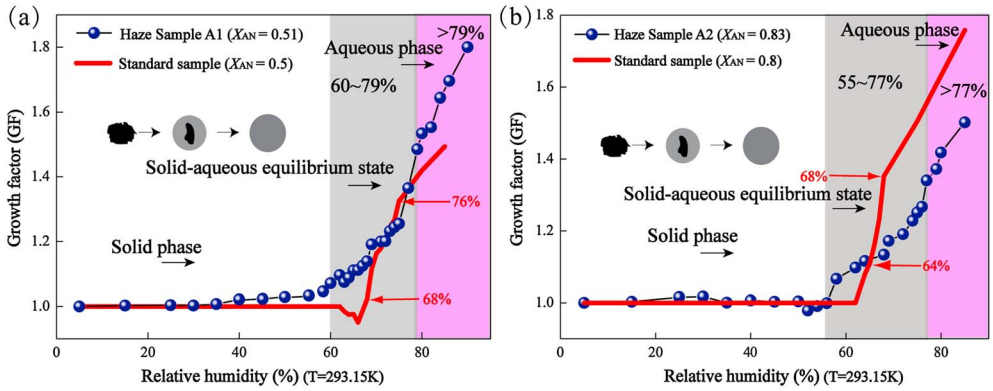

Figure 5. Hygroscopic growth factor curves of haze sample A1 (X_{AN} = 0.51) and A2 (X_{AN} = 0.83) particles as a function of RH and comparison with laboratory-generated samples X_{AN} = 0.5 and X_{AN} = 0.8, respectively (T = 293.15 K). Blue circles represent haze samples during hydration process. Red line represents laboratory-generated AS-AN particles' growth curve. Solid phase in blank (A1: RH < 60%; A2: RH < 55%); solid-aqueous equilibrium physical state in gray shadow (A1: RH = 60–79%; A2: RH = 55–77%); aqueous phase in pink shadow (A1: RH > 79%; A2: RH > 77%).

RH = 60% in sample A1 (Figures 5a and 6A1b) and at RH = 55% in sample A2 (Figures 5b and 6A2b). Particles in sample A1 were in solid-aqueous equilibrium state at the RH range of 60–79%, and all particles completely changed into the aqueous phase at RH = 79% (Figures 5a and 6A1c–e). In sample A2, haze particles in solid-aqueous equilibrium state were observed in the RH range of 55–77%, and full deliquescence occurred at RH = 77% (Figures 5b and 6A2c–e). Therefore, haze particles displayed a

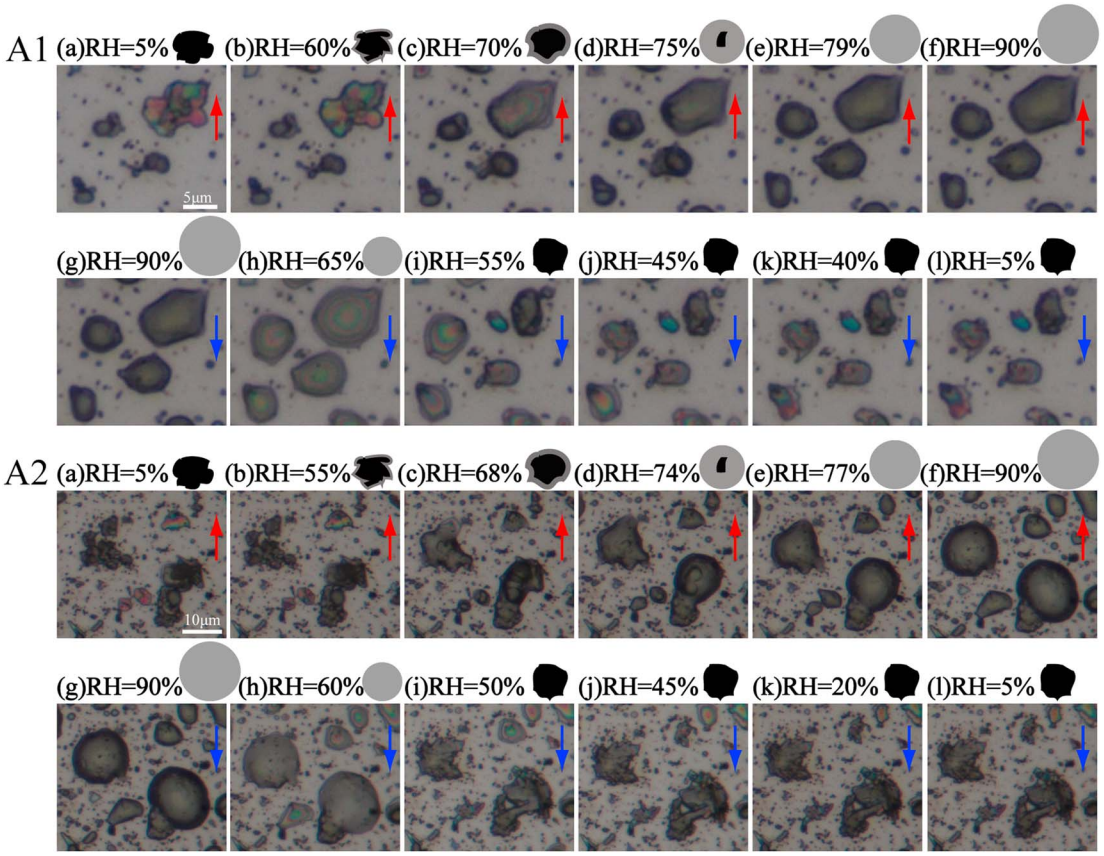

Figure 6. Optical images of haze particle samples A1 and A2 in different RH at T = 293.15 K. (a–f) Particles' hygroscopic growth during hydration process from 5% to 90% RH. Up arrow (↑) represents RH increase; (g–l) Particles' shrinkage during dehydration processes from 90% to 5% RH in the same image field. Down arrow (↓) represents RH decrease.

solid-aqueous equilibrium state when RH was around 60–80% during hydration. During dehydration, particle size decreased gradually with the decrease of RH, but the phase remained aqueous until RH = 55% for sample A1 and 50% for sample A2 (Figures 6A1i and 6A2i). These measured values are higher than laboratory-generated samples X_{AN} = 0.5 and X_{AN} = 0.8, respectively. The reason could be attributed to insoluble core particles (e.g., Figure S2), which serve as heterogeneous nuclei to induce efflorescence at RH higher than ERH of pure salt particles (Cziczo & Abbatt, 2000; Dougle et al., 1998). Soluble organics such as succinic, malonic, and glutaric acids also can induce earlier efflorescence at higher RH. Due to the one-stage efflorescence of haze particles, we deduced that particles kept aqueous phase until RH dropped down to around 50%.

Figures 5a and 5b show that urban haze particles in samples A1 (X_{AN} = 0.51) and A2 (X_{AN} = 0.83) had similar growth curves with AS-AN particles at X_{AN} = 0.5 and X_{AN} = 0.8. We noticed that haze particles had smaller MDRH (60% and 55%) and higher DRH (79% and 77%) compared to laboratory-generated AS-AN particles (X_{AN} = 0.5, MDRH = 68% and DRH = 76%; X_{AN} = 0.8, MDRH = 64% and DRH = 68%). TEM observations showed that inorganic components in individual particles were coated by or mixed with organic matter (Figure S2). This phenomenon might be attributed to organic matter mixed with AS and AN. Some studies reported that secondary organic aerosols within individual inorganic particles can induce particles to start to deliquesce at lower RH (i.e., MDRH) and completely deliquesce at higher RH (i.e., DRH; Peckhaus et al., 2012; Smith et al., 2012; Wu et al., 2011). In a word, our results illustrate that the AN content in individual haze particles plays an important role in determining their MDRH and that the AS content significantly affects their DRH.

3.4. Atmospheric Implications

RH is a critical factor in determining the phase of haze particles in north China. We statistically analyzed RH during haze episodes at the sampling site in 2015 (Figure S3), 33% of haze episodes occurred at RH below 50%, 18% at RH of 50–60%, 35% at RH of 60–80%, and 14% of them occurred at RH above 80%. Therefore, haze particles dominated by AS-AN mainly existed as the mixed solid-aqueous equilibrium physical state and aqueous phase in the polluted air of urban north China. To the best of our knowledge, our study is the first to provide direct evidence that most haze particles exist as a solid core coated with an aqueous shell in polluted air.

The heterogeneous reaction rates on particle surfaces have been assumed to depend on RH (Stutz et al., 2004). Model studies for haze formation and evolution until now simply concluded that the gas uptake coefficient remained at its lower limit when RH $\leq$ 50% and increased linearly with RH increase (B. Zheng et al., 2015; Cheng et al., 2016; Y. Wang et al., 2014), ignoring the complicated phase changes of individual particles. Chen et al. (2016) proposed that the underestimation of heterogeneous reaction rates that were related to underestimated uptake coefficient at 60–90% RH was a significant reason for the underprediction of the peak $PM_{2.5}$ concentrations. We believe that the biases between field observation and model simulations may be attributed to neglecting the occurrence of phase changes. Based on our study, most urban haze particles with aqueous shells at RH = 60–80% provide an important reactive surface for heterogeneous reactions of trace gases, which accelerate the haze formation. In northern China, some morning fog can develop into haze episodes in daytime in the winter (Yuan et al., 2015). The fog-haze conversion displays RH from 90–100% down to 60%, but these suspended aerosol particles still remain in the aqueous phase during the haze episodes until the RH drops down to ~50%. These aqueous aerosol particles immediately provided important reactive surfaces for transformation of NO_2, SO_2, and VOCs in the haze.

Following the control of sulfur dioxide pollution in China, recent studies found that nitrate concentrations in $PM_{2.5}$ increased and sulfate decreased (Lu et al., 2015; Yang et al., 2015; X. Y. Zhang et al., 2015). According to our study, aerosol particles will be more hygroscopic and deliquesce earlier as molar ratio of AN to AS increases. Moreover, visibility significantly decreased with RH increase during the haze because shape changes of the deliquesced particles had a significant influence on light scattering (Freney et al., 2010). Adachi et al. (2011) showed that atmospheric particles with a solid core in a liquid shell can scatter light up to 50% more efficiently when compared to the conventional assumption that all particles are liquid after a given RH. Additional studies on heterogeneous reaction rates related to different particle phases, especially solid-aqueous equilibrium state at RH 60–80% RH and aqueous phase at RH $>$ 80%, are needed for a better prediction of haze formation in China by chemical transport models.

Acknowledgments
We thank Peter Hyde and Bingbing Wang's comments and proofreading. This work was funded by the National Key R&D Program of China (2017YFC0212700), National Natural Science Foundation of China (41575116, 41622504), and the Hundred Talents Program in Zhejiang University. All data displayed in figures is available on Github at https://github.com/liwjatmos/JGRD54383-database.

References

Adachi, K., Freney, E. J., & Buseck, P. R. (2011). Shapes of internally mixed hygroscopic aerosol particles after deliquescence, and their effect on light scattering. *Geophysical Research Letters*, *38*, L13804. https://doi.org/10.1029/2011GL047540

Ahn, K. H., Kim, S. M., Jung, H. J., Lee, M. J., Eom, H. J., Maskey, S., & Ro, C. U. (2010). Combined use of optical and electron microscopic techniques for the measurement of hygroscopic property, chemical composition, and morphology of individual aerosol particles. *Analytical Chemistry*, *82*, 7999–8009. https://doi.org/10.1021/ac101432y

Chen, D., Liu, Z., Fast, J., & Ban, J. (2016). Simulations of sulfate–nitrate–ammonium (SNA) aerosols during the extreme haze events over northern China in October 2014. *Atmospheric Chemistry and Physics*, *16*(16), 10,707–10,724. https://doi.org/10.5194/acp-16-10707-2016

Cheng, Y., Zheng, G., Wei, C., Mu, Q., Zheng, B., Wang, Z., … Carmichael, G. (2016). Reactive nitrogen chemistry in aerosol water as a source of sulfate during haze events in China. *Science Advances*, *2*(12), e1601530. https://doi.org/10.1126/sciadv.1601530

Clegg, S. L., Brimblecombe, P., & Wexler, A. S. (1998). Thermodynamic model of the system H^+-NH_4^+-SO_4^{2-}-NO^{3-}-H_2O at tropospheric temperatures. *The Journal of Physical Chemistry. A*, *102*(12), 2137–2154. https://doi.org/10.1021/jp973042r

Cziczo, D. J., & Abbatt, J. P. D. (2000). Infrared observations of the response of NaCl, $MgCl_2$, NH_4HSO_4, and NH_4NO_3 aerosols to changes in relative humidity from 298 to 238 K. *The Journal of Physical Chemistry. A*, *104*(10), 2038–2047. https://doi.org/10.1021/jp9931408

Dougle, P. G., Veefkind, J. P., & Brink, H. M. T. (1998). Crystallisation of mixtures of ammonium nitrate, ammonium sulphate and soot. *Journal of Aerosol Science*, *29*(3), 375–386. https://doi.org/10.1016/S0021-8502(97)10003-9

Ervens, B. (2015). Modeling the processing of aerosol and trace gases in clouds and fogs. *Chemical Reviews*, *115*(10), 4157–4198. https://doi.org/10.1021/cr5005887

Fairlie, T. D., Jacob, D. J., Dibb, J. E., Alexander, B., Avery, M. A., Donkelaar, A. V., & Zhang, L. (2010). Impact of mineral dust on nitrate, sulfate, and ozone in transpacific Asian pollution plumes. *Atmospheric Chemistry and Physics*, *10*, 3999–4012. https://doi.org/10.5194/acp-10-3999-2010

Fong, B. N., Kennon, J. T., & Ali, H. M. (2016). Mole ratio dependence of the mutual deliquescence relative humidity of aqueous salts of atmospheric importance. *The Journal of Physical Chemistry. A*, *120*(20), 3596–3601. https://doi.org/10.1021/acs.jpca.6b02706

Freney, E. J., Adachi, K., & Buseck, P. R. (2010). Internally mixed atmospheric aerosol particles: Hygroscopic growth and light scattering. *Journal of Geophysical Research*, *115*, D19210. https://doi.org/10.1029/2009JD013558

Ge, Z. Z., Wexler, A. S., & Johnston, M. V. (1998). Deliquescence behavior of multicomponent aerosols. *The Journal of Physical Chemistry. A*, *102*(1), 173–180. https://doi.org/10.1021/jp972396f

Gupta, D., Kim, H., Park, G., Li, X., Eom, H. J., & Ro, C. U. (2015). Hygroscopic properties of NaCl and $NaNO_3$ mixture particles as reacted inorganic sea-salt aerosol surrogates. *Atmospheric Chemistry and Physics*, *15*(6), 3379–3393. https://doi.org/10.5194/acp-15-3379-2015

Hodas, N., Sullivan, A. P., Skog, K., Keutsch, F. N., Collett, J. L., Decesari, S., … Turpin, B. J. (2014). Aerosol liquid water driven by anthropogenic nitrate: Implications for lifetimes of water-soluble organic gases and potential for secondary organic aerosol formation. *Environmental Science & Technology*, *48*(19), 11127–11136. https://doi.org/10.1021/es5025096

Hodas, N., Zuend, A., Mui, W., Flagan, R. C., & Seinfeld, J. H. (2014). Influence of particle-phase state on the hygroscopic behavior of mixed organic-inorganic aerosols. *Atmospheric Chemistry and Physics*, *15*(9), 5027–5045.

Hu, D., Chen, J., Ye, X., Li, L., & Yang, X. (2011). Hygroscopicity and evaporation of ammonium chloride and ammonium nitrate: Relative humidity and size effects on the growth factor. *Atmospheric Environment*, *45*, 2349–2355. https://doi.org/10.1016/j.atmosenv.2011.02.024

Huang, R. J., Zhang, Y., Bozzetti, C., Ho, K. F., Cao, J. J., Han, Y., … Prevot, A. S. H. (2014). High secondary aerosol contribution to particulate pollution during haze events in China. *Nature*, *514*(7521), 218–222. https://doi.org/10.1038/nature13774

Jing, B., Tong, S., Liu, Q., Li, K., Wang, W., Zhang, Y., & Ge, M. (2016). Hygroscopic behavior of multicomponent organic aerosols and their internal mixtures with ammonium sulfate. *Atmospheric Chemistry and Physics*, *16*(6), 4101–4118. https://doi.org/10.5194/acp-16-4101-2016

Kuang, Y., Zhao, C. S., Ma, N., Liu, H. J., Bian, Y. X., Tao, J. C., & Hu, M. (2016). Deliquescent phenomena of ambient aerosols on the North China Plain. *Geophysical Research Letters*, *43*, 8744–8750. https://doi.org/10.1002/2016GL070273

Laskina, O., Morris, H. S., Grandquist, J. R., Qin, Z., Stone, E. A., Tivanski, A. V., & Grassian, V. H. (2015). Size matters in the water uptake and hygroscopic growth of atmospherically relevant multicomponent aerosol particles. *The Journal of Physical Chemistry. A*, *119*(19), 4489–4497. https://doi.org/10.1021/jp510268p

Li, W. J., Zhou, S. Z., Wang, X. F., Xu, Z., Yuan, C., Yu, Y. C., … Wang, W. X. (2011). Integrated evaluation of aerosols from regional brown hazes over northern China in winter: Concentrations, sources, transformation, and mixing states. *Journal of Geophysical Research*, *116*, D09301. https://doi.org/10.1029/2010JD015099

Li, W. J., Sun, J. X., Xu, L., Shi, Z. B., Riemer, N., Sun, Y. L., … Wang, X. F. (2016). A conceptual framework for mixing structures in individual aerosol particles. *Journal of Geophysical Research: Atmospheres*, *121*, 13,784–13,798. https://doi.org/10.1002/2016JD025252

Liu, H. J., Zhao, C. S., Nekat, B., Ma, N., Wiedensohler, A., van Pinxteren, D., … Herrmann, H. (2014). Aerosol hygroscopicity derived from size-segregated chemical composition and its parameterization in the North China Plain. *Atmospheric Chemistry and Physics*, *14*(5), 2525–2539. https://doi.org/10.5194/acp-14-2525-2014

Lu, Y., Chi, J., Yao, L., Yang, L., Li, W., Wang, Z., & Wang, W. (2015). Composition and mixing state of water soluble inorganic ions during hazy days in a background region of north China. *Science China Earth Sciences*, *58*(11), 2026–2033. https://doi.org/10.1007/s11430-015-5131-5

Martin, S. T. (2000). Phase transitions of aqueous atmospheric particles. *Chemical Reviews*, *100*(9), 3403–3454. https://doi.org/10.1021/cr990034t

Mikhailov, E., Vlasenko, S., Niessner, R., & Pöschl, U. (2004). Interaction of aerosol particles composed of protein and salts with water vapor: Hygroscopic growth and microstructural rearrangement. *Atmospheric Chemistry and Physics*, *4*, 323–350. https://doi.org/10.5194/acp-4-323-2004

Morris, H. S., Estillore, A. D., Laskina, O., Grassian, V. H., & Tivanski, A. V. (2016). Quantifying the hygroscopic growth of individual submicrometer particles with atomic force microscopy. *Analytical Chemistry*, *88*(7), 3647–3654. https://doi.org/10.1021/acs.analchem.5b04349

Onasch, T. B., Siefert, R. L., Brooks, S. D., Prenni, A. J., Murray, B., Wilson, M. A., & Tolbert, M. A. (1999). Infrared spectroscopic study of the deliquescence and efflorescence of ammonium sulfate aerosol as a function of temperature. *Journal of Geophysical Research*, *104*(D17), 21,317–21,326. https://doi.org/10.1029/1999JD900384

Peckhaus, A., Grass, S., Treuel, L., & Zellner, R. (2012). Deliquescence and efflorescence behavior of ternary inorganic/organic/water aerosol particles. *The Journal of Physical Chemistry. A*, *116*, 6199–6210. https://doi.org/10.1021/jp211522t

Smith, M. L., Bertram, A. K., & Martin, S. T. (2012). Deliquescence, efflorescence, and phase miscibility of mixed particles of ammonium sulfate and isoprene-derived secondary organic material. *Atmospheric Chemistry and Physics*, *12*, 9613–9628. https://doi.org/10.5194/acp-12-9613-2012

Stutz, J., Alicke, B., Ackermann, R., Geyer, A., Wang, S., White, A. B., … Fast, J. D. (2004). Relative humidity dependence of HONO chemistry in urban areas. *Journal of Geophysical Research*, *109*, D03307. https://doi.org/10.1029/2003JD004135

Sun, Y. L., Wang, Z. F., Fu, P. Q., Yang, T., Jiang, Q., Dong, H. B., … Jia, J. J. (2013). Aerosol composition, sources and processes during wintertime in Beijing, China. *Atmospheric Chemistry and Physics*, *13*(9), 4577–4592. https://doi.org/10.5194/acp-13-4577-2013

Wang, Y., Zhang, Q., Jiang, J., Wei, Z., Wang, B., He, K., … Xie, Y. (2014). Enhanced sulfate formation during China's severe winter haze episode in Jan 2013 missing from current models. *Journal of Geophysical Research: Atmospheres*, *119*, 10,425–10,440. https://doi.org/10.1002/2013JD021426

Wang, X., Ye, X., Chen, H., Chen, J., Yang, X., & Gross, D. S. (2014). Online hygroscopicity and chemical measurement of urban aerosol in Shanghai, China. *Atmospheric Environment*, *95*(1), 318–326. https://doi.org/10.1016/j.atmosenv.2014.06.051

Wang, G., Zhang, R., Gomez, M. E., Yang, L., Zamora, M. L., Hu, M., … Hu, T. (2016). Persistent sulfate formation from London Fog to Chinese haze. *Proceedings of the National Academy of Sciences of the United States of America*, *113*(48), 13,630–13,635. https://doi.org/10.1073/pnas.1616540113

Wexler, A. S., & Seinfeld, J. H. (1991). Second-generation inorganic aerosol model. *Atmospheric Environment*, *25*(12), 2731–2748. https://doi.org/10.1016/0960-1686(91)90203-J

Wise, M. E., Martin, S. T., Russell, L. M., & Buseck, P. R. (2008). Water uptake by NaCl particles prior to deliquescence and the phase rule. *Aerosol Science and Technology*, *42*, 281–294. https://doi.org/10.1080/02786820802047115

Wise, M. E., Freney, E. J., Tyree, C. A., Allen, J. O., Martin, S. T., Russell, L. M., & Buseck, P. R. (2009). Hygroscopic behavior and liquid-layer composition of aerosol particles generated from natural and artificial seawater. *Journal of Geophysical Research*, *114*, D03201. https://doi.org/10.1029/2008JD010449

Wu, Z. J., Nowak, A., Poulain, L., Herrmann, H., & Wiedensohler, A. (2011). Hygroscopic behavior of atmospherically relevant water-soluble carboxylic salts and their influence on the water uptake of ammonium sulfate. *Atmospheric Chemistry and Physics*, *11*, 12,617–12,626. https://doi.org/10.5194/acp-11-12617-2011

Yang, Y. R., Liu, X. G., Qu, Y., An, J. L., Jiang, R., Zhang, Y. H., … Ma, Q. X. (2015). Characteristics and formation mechanism of continuous hazes in China: A case study during the autumn of 2014 in the North China Plain. *Atmospheric Chemistry and Physics*, *15*(14), 8165–8178. https://doi.org/10.5194/acp-15-8165-2015

Yuan, Q., Li, W., Zhou, S., Yang, L., Chi, J., Sui, X., & Wang, W. (2015). Integrated evaluation of aerosols during haze-fog episodes at one regional background site in North China Plain. *Atmospheric Research*, *156*(1), 102–110. https://doi.org/10.1016/j.atmosres.2015.01.002

Zardini, A. A., Sjogren, S., Marcolli, C., Krieger, U. K., Gysel, M., Weingartner, E., … Peter, T. (2008). A combined particle trap/HTDMA hygroscopicity study of mixed inorganic/organic aerosol particles. *Atmospheric Chemistry and Physics*, *8*, 5589–5601. https://doi.org/10.5194/acp-8-5589-2008

Zhang, X. Y., Wang, J. Z., Wang, Y. Q., Liu, H. L., Sun, J. Y., & Zhang, Y. M. (2015). Changes in chemical components of aerosol particles in different haze regions in China from 2006 to 2013 and contribution of meteorological factors. *Atmospheric Chemistry and Physics*, *15*(22), 12,935–12,952. https://doi.org/10.5194/acp-15-12935-2015

Zhang, L., Sun, J. Y., Shen, X. J., Zhang, Y. M., Che, H., Ma, Q. L., … Ogren, J. A. (2015). Observations of relative humidity effects on aerosol light scattering in the Yangtze River Delta of China. *Atmospheric Chemistry and Physics*, *15*(14), 8439–8454. https://doi.org/10.5194/acp-15-8439-2015

Zheng, B., Zhang, Q., Zhang, Y., He, K. B., Wang, K., Zheng, G. J., … Kimoto, T. (2015). Heterogeneous chemistry: A mechanism missing in current models to explain secondary inorganic aerosol formation during the January 2013 haze episode in north China. *Atmospheric Chemistry and Physics*, *15*(4), 2031–2049. https://doi.org/10.5194/acp-15-2031-2015

Zheng, G. J., Duan, F. K., Su, H., Ma, Y. L., Cheng, Y., Zheng, B., … He, K. B. (2015). Exploring the severe winter haze in Beijing: The impact of synoptic weather, regional transport and heterogeneous reactions. *Atmospheric Chemistry and Physics*, *15*(6), 2969–2983. https://doi.org/10.5194/acp-15-2969-2015